IOP-Induced Lamina Cribrosa Deformation and Scleral Canal Expansion: Independent or Related?

Ian A. Sigal,[1] *Hongli Yang,*[2] *Michael D. Roberts,*[1] *Jonathan L. Grimm,*[1,2] *Claude F. Burgoyne,*[2] *Shaban Demirel,*[3] *and J. Crawford Downs*[1]

Purpose. To study the association between the intraocular pressure (IOP)–induced anterior–posterior lamina cribrosa deformation (LCD) and scleral canal expansion (SCE).

Methods. 3D eye-specific models of the lamina and sclera of the eyes of three normal monkeys were constructed. Morphing techniques were used to produce 768 models with controlled variations in geometry and materials. Finite element analysis was used to predict the LCD and SCE resulting from an increase in IOP. We analyzed the association between LCD and SCE for the population as a whole, and for subsets.

Results. For some conditions, such as deep and stiff lamina, the association between LCD and SCE was strong and consistent with the concept of "the sclera pulls the lamina taut" as IOP increases. For other conditions, such as shallow and compliant lamina, there was no association. Further, for other conditions, such as for thin and stiff sclera, the association was opposite to the tautening. Although most of the models had similar response to IOP, some cases had peculiarly large LCD and SCE. The properties of the lamina cribrosa (LC) greatly influenced its response to variations in IOP; for example, deep laminas tended to displace anteriorly, whereas shallow LCs displaced little or posteriorly.

Conclusions. The association between LCD and SCE varied greatly depending on the properties of the lamina and sclera, which shows that it is critical to consider the characteristics of the population when interpreting measurements of LCD and SCE. This work is the first systematic analysis of the relationship between LCD and SCE. (*Invest Ophthalmol Vis Sci.* 2011; 52:9023–9032) DOI:10.1167/iovs.11-8183

Glaucoma, one of the leading causes of blindness worldwide,[1] is generally regarded to result from damage to the retinal ganglion cell axons as they traverse the lamina cribrosa (LC), a structure within the optic nerve head (ONH).[2] Although lowering intraocular pressure (IOP) remains the only proven method for preventing or delaying the onset and progression of glaucomatous vision loss, the role of IOP in the neuropathy remains unclear.[3–5] This is, at least in part, due to the wide spectrum of individual sensitivity to IOP, wherein significant numbers of individuals with normal IOP develop glaucoma (e.g., normotensive glaucoma), whereas other individuals with elevated IOP show no signs of the disease (e.g., ocular hypertensive).[3,4,6] Diagnosis and treatment would benefit from an improved understanding of the effects of IOP on the ONH, and of the factors determining individual sensitivity to IOP. The deformations of the LC produced by variations in IOP have thus been studied with numerical[7–14] and experimental[15–20] techniques.

Consensus is emerging within the ocular biomechanics literature that the lamina cribrosa does not respond to changes in IOP in isolation, but rather that the ONH and peripapillary sclera behave as a mechanical system (Fig. 1).[4,5,7,9,10,12,17,18,20] The primary objective of this work was to study the relationship between the anterior–posterior lamina cribrosa deformation (LCD) and scleral canal expansion (SCE) produced by an IOP increase.[21] To the best of our knowledge, although several studies have proposed this relationship,[4,5,7,9,10,12,17,18,21,22] no study has explored it methodically. Identifying associations between responses to IOP has been a challenge because these result from a complex nonlinear combination of factors, including two- and three-factor interactions.[12,21] Ultimately, however, the ability to determine the mechanical sensitivity to IOP of a particular ONH will benefit from an improved understanding of how the factors combine.

In this article we describe the results of a study wherein we used parameterized eye-specific finite element models of normal monkey eyes to predict the IOP-induced LCD and SCE for 768 models of the ONH, with varying tissue mechanical properties and geometries. We analyzed the model predictions to determine whether there is an association between LCD and SCE and, if so, under which conditions. We also analyzed the predicted LCD and SCE to identify ONH characteristics that lead to peculiarly large LCD and SCE, which indicates increased biomechanical sensitivity to IOP.

Methods

Model preparation and simulation of their response to increases in IOP was as described elsewhere.[21] This analysis, however, has some important differences: whereas we previously studied the population of models as a whole using statistical analysis techniques to gain "forest-level" understanding, in this work we have studied subsets of models, sometimes as small as an individual case to gain "tree-level" insight. The strategy was to construct 3D eye-specific baseline models of the lamina and sclera of both eyes of three normal monkeys. The geometry and material properties of each baseline model were parameterized using morphing techniques.[23,24] This enabled us to produce 768 new "morphed" models related to the baseline models with precisely controlled variations in geometry and materials by specifying a few high-level parameters, or factors. Finite element analysis was used in each model to predict the LCD and SCE resulting from an increase in

From the [1]Ocular Biomechanics Laboratory, the [2]Optic Nerve Head Research Laboratory, and the [3]Perimetry and Psychophysics Laboratory, Devers Eye Institute, Portland, Oregon.

Supported in part by National Institutes of Health Grants R01-EY18926, R01-EY19333, and R01-EY11610; and Biomedical Research Infrastructure Network/IDeA Networks of Biomedical Research Excellence Grant P20 RR16456.

Submitted for publication July 7, 2011; accepted August 31, 2011.

Disclosure: **I.A. Sigal**, None; **H. Yang**, None; **M.D. Roberts**, None; **J.L. Grimm**, None; **C.F. Burgoyne**, None; **S. Demirel**, none; **J.C. Downs**, None

Corresponding author: Ian A. Sigal, Department of Ophthalmology, University of Pittsburgh, 203 Lothrop St., Room 930, Pittsburgh, PA 15213; sigalia@upmc.edu.

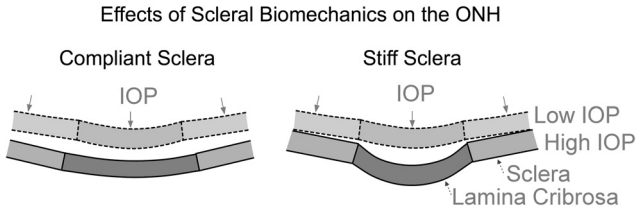

FIGURE 1. Schematic representation of how the deformations of the sclera and lamina may be related. When describing the effects of IOP on the LC, a useful conceptual framework has emerged in the last few years: that of the balance between the direct effects of IOP "pushing" the lamina posteriorly, and the indirect effects of IOP deforming the sclera, expanding the canal, which in turn "pulls" the lamina taut from the sides.[4,9,13,14,17,18,21,22,29,34,35] A stiff sclera deforms little under IOP (*right*), with a small SCE, allowing the lamina to be displaced posteriorly by the action of IOP on its anterior surface. Conversely, in the case of a compliant sclera (*left*), an increase in IOP induces large scleral deformations, which are transmitted to the scleral canal, resulting in a large SCE that pulls the lamina taut. Tautening of the lamina reduces posterior LCD or even results in anterior LCD, despite the effects of IOP on the LC (adapted from Sigal and Ethier[5]).

IOP.[25,26] We analyzed the association between LCD and SCE for all the models and subsets, and identified combinations of factors with particularly large LCD and SCE.

Model Preparation and Simulation

Details of tissue preparation, baseline model reconstruction, model parameterization, discretization (meshing), and simulation are given elsewhere.[10,11,21,23] In the following text we provide only a brief description of these methods.

The models were reconstructed from manual delineations of the neural canal wall, and the anterior and posterior surfaces of the lamina cribrosa and peripapillary sclera, done on serial stained block-face images of eyes perfusion-fixed at an IOP of 10 mm Hg. All animals were treated in accordance with the ARVO Resolution on the Use of Animals in Ophthalmic and Vision Research.

Morphing techniques were used to parameterize five geometric characteristics of the models: lamina cribrosa thickness and position,

TABLE 1. Factors Studied and Their Levels

Factor	Factor Range	
	Low	**High**
Geometry		
Scleral canal radius, μm	569	787
Scleral canal eccentricity	1.24	1.57
Scleral thickness, μm	116	217
Lamina cribrosa thickness, μm	82	150
Lamina cribrosa position, μm	42	152
Mechanical properties		
Scleral modulus, MPa	5.3	18.4
Lamina cribrosa modulus, MPa	0.39	3.7
Individual eye		
Eye	Nominal categorical factor with 6 levels, one for each eye-specific model parameterized.	

The ranges over which the geometric factors were varied were obtained from 3D histomorphometry of 21 normal monkey eyes (including those in this study).[17,27–29] See Figure 2 for an illustration of the geometries produced by varying the factors to low and high levels.

scleral canal size and eccentricity, and scleral thickness. Geometric parameter ranges were obtained from 3D histomorphometry of 21 normal monkey eyes (including those in this study),[18,27–29] and are listed in Table 1, and illustrated in Figure 2. Intereye geometric variability was parameterized by defining eye as a nominal categorical factor with six levels, one for each eye-specific baseline model. Two material mechanical properties were parameterized following the same strategy and rationale described and discussed in Sigal et al.[21] All tissues were assumed to be linearly elastic, isotropic, and homogeneous, with their mechanical behavior determined by their Young's moduli, which we parameterized, and their Poisson ratio, which we kept constant at 0.45 (close to the incompressible limit of 0.5 for this type of material). Material properties were not derived from the same eyes, yet are among the most influential factors on the response to IOP.[10,12–14,21,30,31] Thus, we replicated the study, repeating all runs and analyses, using different material property ranges. The choice of

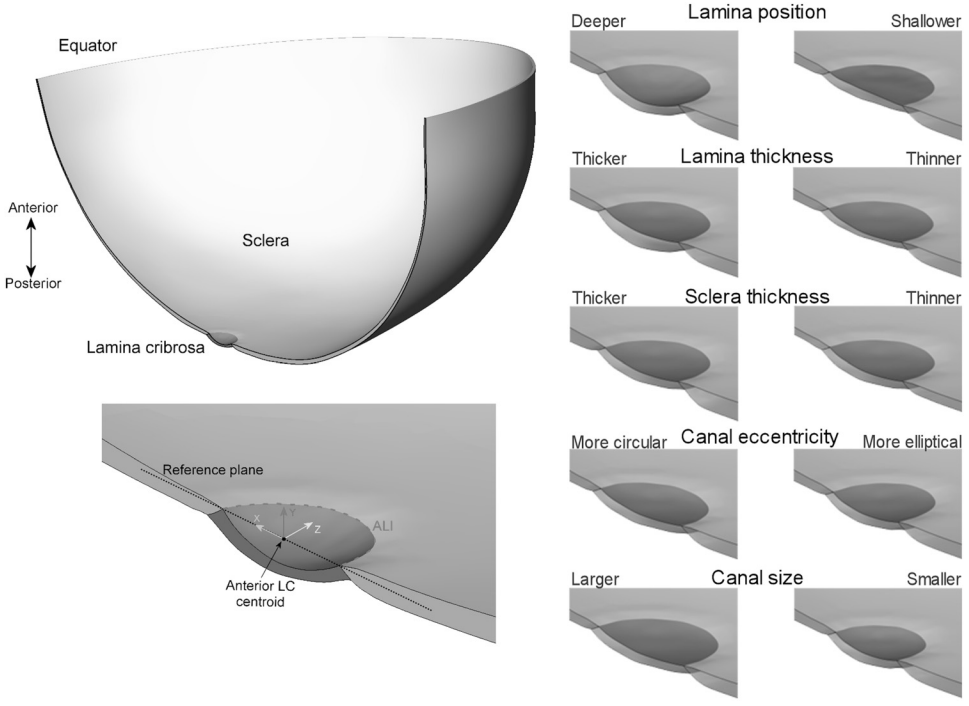

FIGURE 2. Model geometry and examples of geometry variations. *Top left*: Cut-out view of a baseline eye-specific model, with the lamina cribrosa in *blue* and the sclera in *yellow*. *Bottom left*: Detail of the ONH region illustrating the orientation of the LC relative to the system of coordinates, and the reference plane. The reference plane was fit by least-squares to the anterior lamina insertion into the sclera (ALI, *dashed line*), and used to define lamina position. Five features of the model geometry were defined and varied with morphing techniques (*right side*): lamina cribrosa position and thickness, scleral thickness, and scleral canal size and eccentricity. The morphed models are shown at the extremes of the corresponding factor (high on the *left side column*, and low on the *right side column*). LCD was defined as IOP-induced changes of lamina position. SCE was defined as IOP-induced changes in canal size.

ranges affected the predicted LCD and SCE only slightly, and the results remained consistent. For clarity, we show results obtained with laminar properties based on the studies by Roberts et al.,[10,32] and scleral properties as an average of the values from uniaxial[33] and inflation[7,34] tests.

The models were formed by between 100,000 and 230,000 10-node tetrahedral elements, depending on the geometry. The effects of IOP were modeled as a distributed load of 5 mm Hg acting on the element faces exposed to the interior of the eye. The magnitude of these forces was chosen to represent a modest increase in IOP from the eye fixation pressure (10 mm Hg) to an elevated level still within the normal range (15 mm Hg). The rationale for this choice is addressed in the Discussion section. The nodes on the equator were restricted to deform radially on the plane of the equator.

SCE was defined as the change in canal size, computed as the change in mean anterior lamina insertion distance to its centroid. LCD was defined as the change in lamina cribrosa position, computed as the change in mean anterior–posterior position of the anterior lamina surface relative to a least-squares plane fit to the anterior laminar insertion points. Model pre- and postprocessing, including morphing and meshing, were done using a combination of open-source (Python, www.python.org; Python Software Foundation) and commercial software (Amira Dev4.1.1; Visage Imaging, Richmond, VIC, Australia). Finite element simulation was done with commercial software (Abaqus v. 6.8.1; Dassault Systèmes, Vélizy-Villacoublay, France).

Experiment Design and Analysis

The combinations of ONH characteristics were selected according to a two-level full-factorial experimental design, which samples all corners of the seven-dimensional space defined by the continuous factors.[25,26] The design was repeated six times, one for each baseline eye-specific model, resulting in 768 model combinations ($2^7 \times 6 = 768$). This design is balanced, meaning that for every factor there were as many models with a low value as with a high one.

We evaluated the relationship between LCD and SCE in all cases together and split into groups obtained by separating the cases at the midpoint of the factor ranges. This meant that the groups had either one half or one quarter of the cases, depending on whether they were split once (by one factor) or twice (by two factors), respectively. We grouped the cases by lamina cribrosa modulus and position, or by scleral modulus and thickness, because these had the strongest influences on LCD and SCE in the previous study, respectively (see the Appendix).[21] For the whole population or each group we evaluated the relationship between LCD and SCE with both parametric (Pearson's product moment correlation coefficient ρ) and nonparametric (Kendall's rank correlation τ) methods. The rationale for repeating the analysis with both techniques is addressed later in the Discussion section. We also analyzed the data using nonlinear regressions and after transforming the responses to improve their normality and that of their residuals.[25,26] These changes affected only slightly the relationships and their statistical significances, and the main results remained consistent. For clarity, we show the results of linear analyses done on untransformed data. Experiment design and analysis were carried out in commercial (Design-Expert v. 8; Stat-ease, Minneapolis, MN) and open-source software (R software; provided in the public domain by the R Foundation for Statistical Computing, Vienna, Austria; available at www.r-project.org), respectively.

Results

SCE was always positive (scleral canal expanding), whereas LCD was in some cases positive (lamina displacing posteriorly with increased IOP) and in others negative (lamina displacing anteriorly with increased IOP) (Fig. 3). When all the cases were analyzed together there was a statistically significant relationship between LCD and SCE in both parametric ($\rho = -0.113$, $P = 0.0017$) and nonparametric ($\tau = -0.278$, $P < 0.0001$) analyses. A negative association means that increased SCE was associated with reduced posterior LCD or increased anterior LCD, consistent with the conceptual framework in the literature (Fig. 1).[5,7,9,10,12,18] The coefficients and the point spread show that, despite being statistically significant, the relationship between LCD and SCE is not simple, is not well approximated by a linear regression, and that there are several point clusters. To illustrate the nature of the lamina and peripapillary sclera deformations, and how they vary over the scatterplot, we selected six cases with a variety of LCD and SCE combinations along the envelope (Fig. 4).

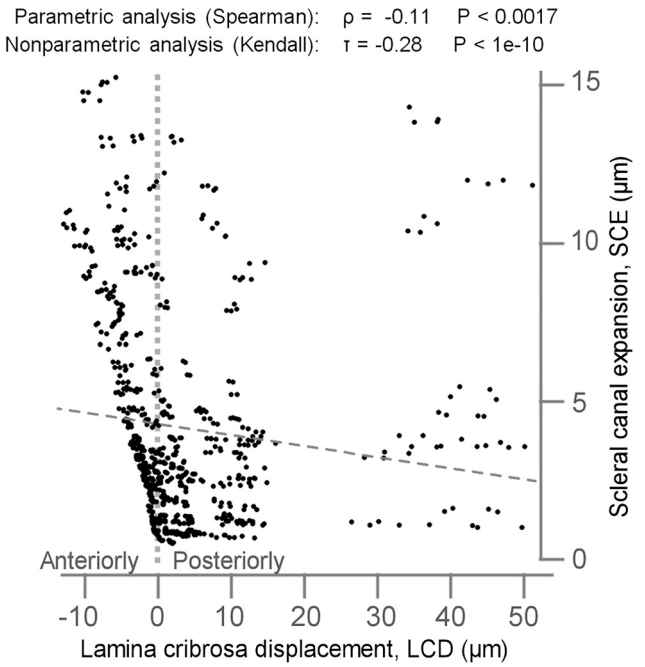

Figure 3. Scatterplot of LCD versus SCE for all cases. Each point represents the LCD and SCE predicted for a given combination of ONH characteristics (one model), and therefore the plot has 768 points. On the *left side* of the *vertical dotted line* are cases where the increase in IOP caused the lamina to displace anteriorly (negative LCD), whereas on the *right* are cases with posterior LCD; 94% of the cases resulted in a small LCD (−15 to 15 μm). Only 6% of the factor combinations resulted in substantial (>20 μm) posterior LCD, and 25% of those also had large (>9 μm) SCE. Notably, there are no points on the *bottom left*, which means that some SCE was necessary for the lamina to displace anteriorly. The framework of a relationship between SCE and LCD described in Figure 1 would appear in this plot as a trend where points on the *right* are lower than points on the *left*, such that increased SCE is associated with decreased posteriorly LCD or increased anteriorly LCD. Both parametric and nonparametric analyses concluded that there was indeed a negative association between LCD and SCE, thus supporting the conceptual framework. The linear regression (*dashed line*) was added to show how the linear fit, although significant, is not a good description of the data, and that there is more to understand of LCD versus SCE than a linear correlation.

How LCD and SCE depend on the factors can be better understood by using scatterplots with the points colored according to the level of a factor (Fig. 5). From such plots it is easy to distinguish the strong sensitivity of LCD to the laminar modulus (Fig. 5E), position (Fig. 5B), and thickness (Fig. 5H), consistent with an analysis of factor influences carried out with purely statistical methods.[21]

By grouping the cases by lamina modulus and position, the two factors with the strongest influences on LCD (Fig. 6), we found that most groups, but not all, had a significant association between LCD and SCE in the direction expected from the conceptual framework. Interestingly, the group with shallow laminas (Fig. 6G) showed a significant association (by the

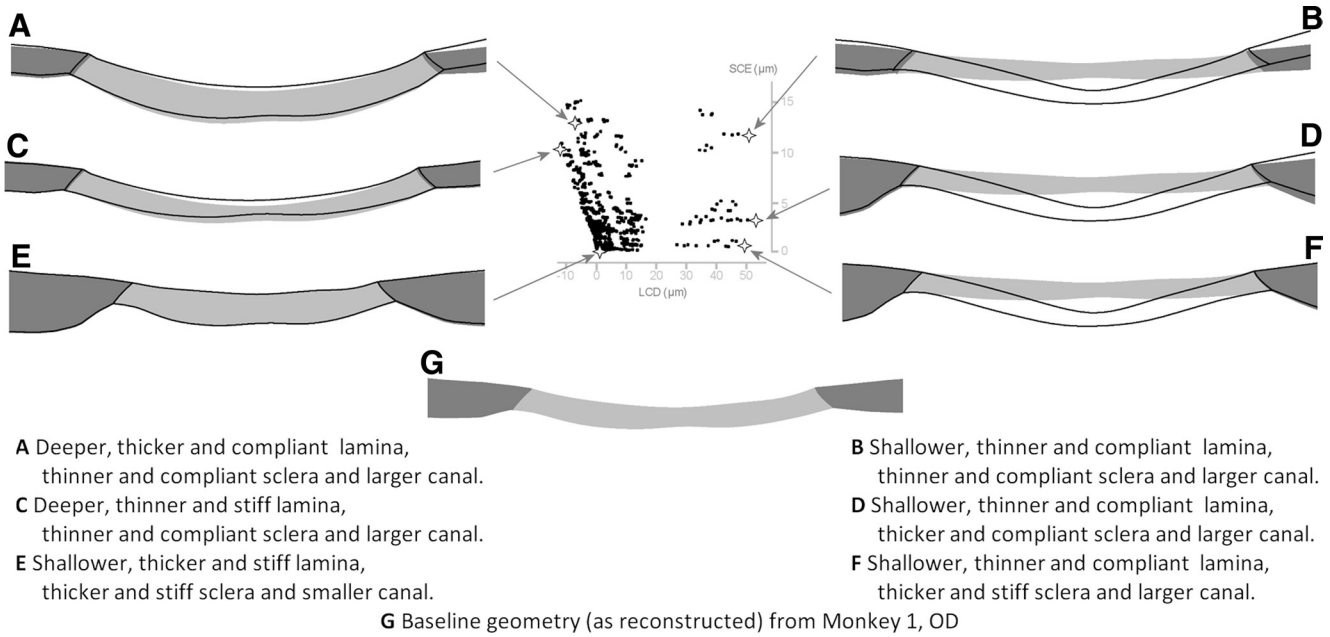

Figure 4. Selected cases with a variety of LCD and SCE combinations. Shown are cross-sections of six models with factors selected to illustrate how these may combine to produce a variety of LCD and SCE. The models (**A–F**) are morphed versions of the eye-specific baseline geometry reconstructed for the OD of monkey 1 (**G**). The *shaded regions* are the undeformed model with the lamina cribrosa in *lighter gray* than the sclera. The *black outlines* show the deformed models, relative to the anterior lamina insertion, with deformations exaggerated fivefold for clarity. In regions with many points we selected a representative example from the many combinations that can produce similar response.

parametric test) in the direction opposite to the conceptual framework (Fig. 1). This illustrates that the association between LCD and SCE depends on the modulus and position of the LC and, furthermore, that these two factors interact.

By grouping the cases by scleral thickness and modulus, the two factors with the strongest influences on SCE (Fig. 7), we found that with the parametric analysis none of the groups or subgroups had a significant association between LCD and SCE in the negative direction expected from the theory. Moreover, one group and three subgroups had a significant positive association. This is interesting because the negative trend in the whole does not exist in any of the subgroups. Results with the nonparametric analysis were mixed: groups with thin and stiff sclera (Fig. 7H) or with thick and soft sclera (Fig. 7F) had a significant positive association, whereas for the other two subgroups the associations were not significant. This emphasizes the importance of using an analysis appropriate to the data.

Discussion

Our goal was to study the association between IOP-induced SCE and LCD, a relationship that has been proposed but never studied methodically. Specifically, we set out to determine whether SCE and LCD are associated and, if so, for which conditions. For this we produced 768 finite element models representing monkey ONHs with varying anatomies and material properties, and analyzed the IOP-induced SCE and LCD predicted for each model. Three main results arise from this study:

1. In many conditions LCD and SCE were associated in a way consistent with the conceptual framework of "the sclera pulls the lamina taut,"[4,9,13,14,17,18,21,22,29,34,35] (i.e., that increased SCE is associated with decreased posterior LCD or even increased anterior LCD).
2. We found the framework to be limited since there were also conditions for which LCD and SCE were not associated and even some conditions in which they were associated, albeit weakly, in a manner opposite to what the framework describes.
3. Although most of the models had somewhat similar responses to IOP, some cases did stand out as having particularly large LCD and SCE. These cases are of interest because they indicate characteristics of the ONH that render it more biomechanically sensitive to acute IOP elevation.

We also confirmed our previous findings that the properties of the LC itself greatly influence its response to variations in IOP.[21] LC position, for example, influences LCD such that deep LCs tended to displace anteriorly, whereas shallow LCs displaced little or posteriorly. Large posterior displacements occurred only in shallow LCs. At first this may appear counterintuitive because it may seem that a lamina that is already "bowed back" would be more likely to keep moving posteriorly than would a lamina that was initially shallow. Our results, however, are in agreement with the measurements of the acute effects of IOP recently reported.[17] Using 3D histomorphometry of contralateral eyes of normal monkeys we found that elevated IOP resulted in anterior LCD in three animals with deep LCs and in posterior LCD in two animals with shallow LCs.[18] Kankipati and colleagues (Kankipati L, et al. *IOVS* 2011; 52:ARVO E-Abstract 6255) analyzed SD-OCT images of healthy human eyes to measure the IOP-induced changes in LC depth with respect to Bruch's membrane opening. They found that the LC displaced anteriorly in younger subjects and posteriorly in older subjects. Our analysis of the data in their poster also shows that shallow LCs (mean depth < 400 μm) were more likely to displace posteriorly (6 of 8 eyes), whereas deep LCs (mean depth > 400 μm) were more likely to displace anteriorly (8 of 10 eyes).

This work is important because it is the first systematic analysis of the relationship between LCD and SCE. Understanding the effects of IOP on the LC is valuable because IOP is the main risk factor for the development and progression of glau-

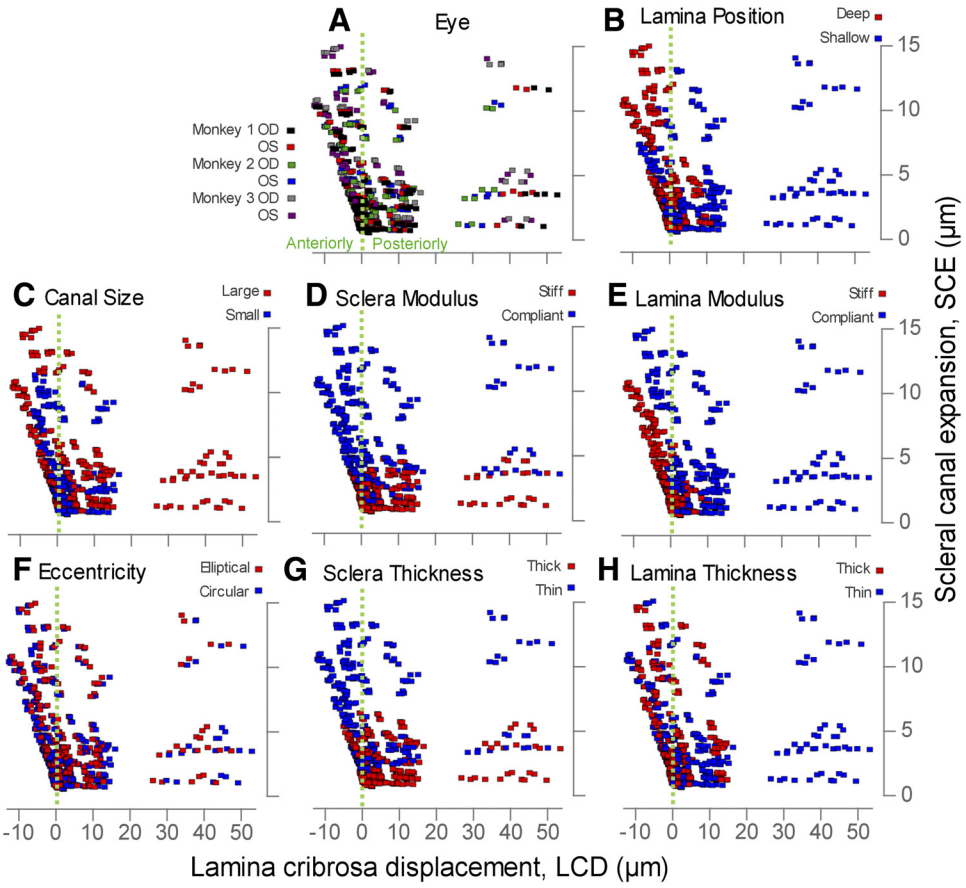

FIGURE 5. SCE versus LCD for all cases colored by each of the parameters. All panels are identical, except for the parameter used to color the symbols. The label above each plot indicates the parameter used to color the points: *red* for high level and *blue* for low level, except for Eye where each eye has a different color. The 12 cases with large LCD and SCE (*top right* of the scatterplots) combined compliant lamina and sclera, thin lamina and sclera, shallow lamina, and large canal size. Anteriorly LCDs were possible, as long as there was some SCE, which occurred most often, but not only, with compliant and thin sclera. The largest anteriorly LCDs occurred for cases with stiff laminas and did not have the largest SCEs. The largest SCEs had compliant and thin sclera, large canal size, and deep and compliant lamina. A thin and more elliptical lamina also increased slightly the maximum SCE, but this effect is probably too small to be important. The differences between the distribution of the points in *blue* and the points in *red* indicate the strength of the parameter or, conversely, the sensitivity of the measure on the parameter. For example, LCD was most sensitive to LC modulus (**E**), position (**B**) thickness (**H**), and canal size (**C**). SCE was most sensitive to sclera modulus (**D**) and thickness (**G**). Both responses were essentially insensitive to canal eccentricity (**F**) and the eye used as baseline (**A**). Since within a panel points with the same color share a particular level of a factor, the spread of points with a given color represents the influence of all other factors. We see, for example, that when the lamina was stiff (*red points*, **E**) the points spread over a smaller range of LCD, than when the lamina was compliant (*blue points*, **E**), and therefore that a stiff lamina reduced the sensitivity of LCD to the other factors. Similarly, the cases with stiff (**D**) or thick sclera (**G**) cover a smaller range on SCE than cases with compliant or thin sclera, again illustrating how these two parameters control, to some extent, the influence of other factors on SCE. A change in the effect of one factor, depending on the level of another factor is an interaction between the two factors.

coma, and because the LC is believed to be the site where damage to the retinal ganglion cell axons initiates.[2–4,6] IOP-induced LCD and SCE, in particular, are receiving increasing attention in the ocular biomechanics community because they represent important components of the LC response to IOP,[4,5] and because these have recently become accessible for in vivo measurement using optical coherence tomography (OCT).[15,20] Until recently, it was thought that increases in IOP caused the LC to deform posteriorly, whereas the sclera remained essentially undeformed.[36] Recent numerical modeling studies, however, predicted that as IOP varies, the sclera deforms, and that these deformations when transmitted to the ONH may have a substantial effect on the deformations of the LC.[12–14,21,22,30,34] In the models, the lateral deformations transmitted by the sclera to the LC could even be larger in magnitude than the anterior–posterior displacements induced by the IOP on the LC.[11,13,21,37] This is consistent with recent measurements obtained using 3D histomorphometry and OCT.[15,17,35] It is now generally accepted that the LC does not respond to IOP changes in isolation, but rather that the ONH and peripapillary sclera behave as a biomechanical system. This association had been described through the conceptual framework of "the sclera pulls the lamina taut" (Fig. 1).

The results we present in this work support this framework, but also that it does not hold in some situations. It is important to note that the exceptions are meaningful from a physiologic perspective. For example, we found that the relationship between LCD and SCE depends on the stiffness and thickness of the sclera (Fig. 7). The sclera of monkeys with experimental glaucoma are stiffer and thicker than those of their normal contralateral eyes.[7,8] Thus, our results suggests that the association between LCD and SCE may be different in glaucomatous monkey eyes with altered connective tissue stiffness when compared with normal eyes.

Notwithstanding the negative association between LCD and SCE in the population as a whole (Fig. 7A), only one of the subgroups obtained by splitting the cases by scleral thickness and modulus shows the negative association between LCD and SCE that is consistent with the proposed framework (Fig. 7F). Furthermore, some of the subgroups had positive associations. It may seem counterintuitive that the combination of subgroups with positive or null trends in each results in a negative trend in the whole. The situation, however, is an example of the Reversal's paradox or Simpson's paradox, which is well understood (Fig. 8).[38,39] This highlights the importance of being careful when either generalizing or particularizing results, and that "Simpson's paradox is not a contrived pedagogical example."[40]

For this particular study we notice that the paradox appears because of the clusters of cases with large LCDs; 6% of the cases yielded large LCDs (48 of 768 ONHs) and one quarter of these (1.5% of the total) also had large SCE. Although these cases are interesting because they have increased biomechani-

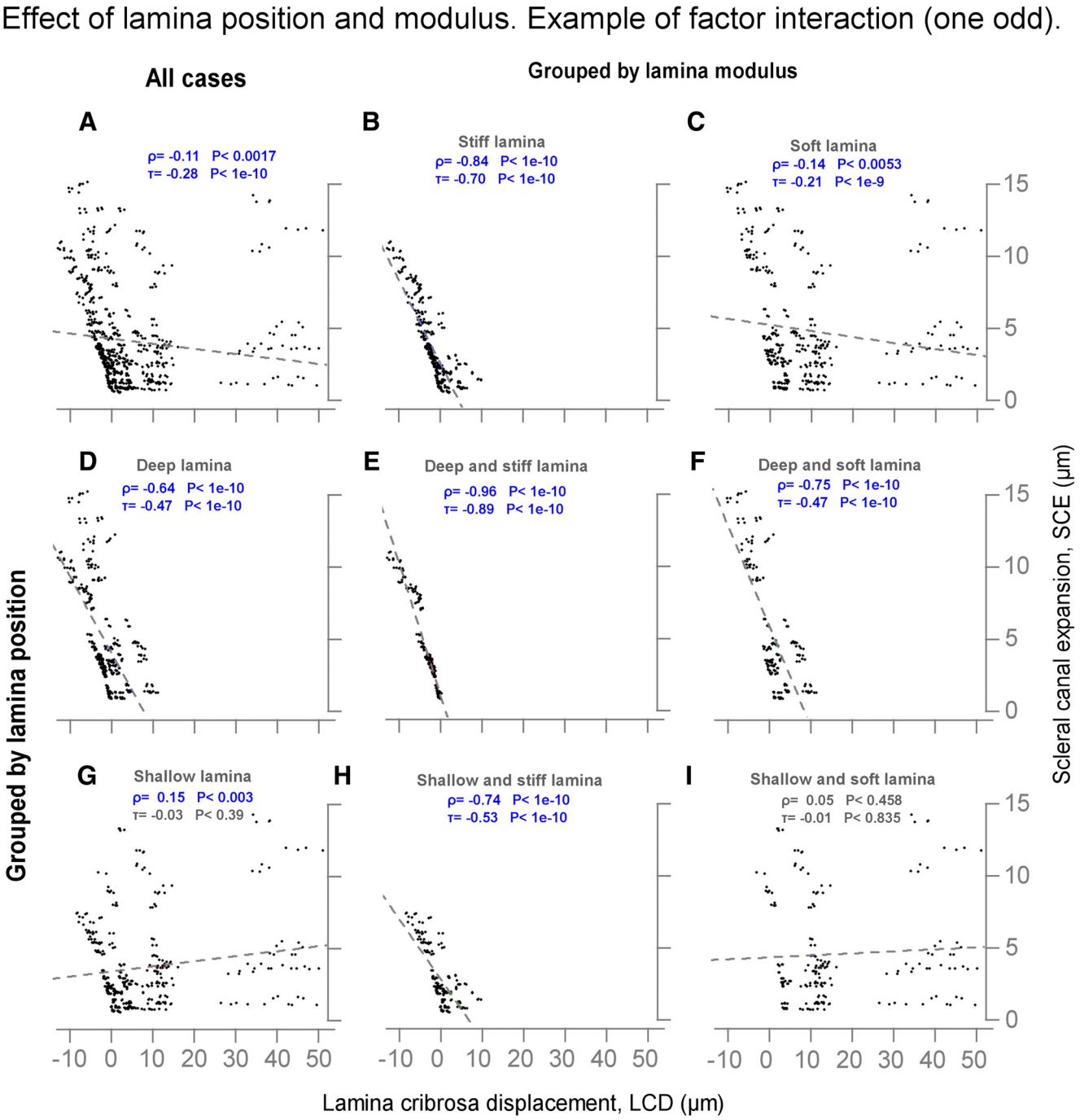

Figure 6. Scatterplot of LCD versus SCE for all cases, and for groups and subgroups split by lamina position and modulus. (**A**) *Top left panel*: Includes all cases and is equivalent to Figure 3. Grouping by one factor, either lamina modulus (**B** and **C**) or position (**D** and **G**), produces groups with statistically significant associations between LCD and SCE. Grouping by modulus produces one strong (**B**) and one weak (**C**) association, both in the direction expected from the conceptual framework above (Fig. 1). Grouping by lamina position results in something surprising: one relatively strong and significant relationship in the expected direction (**D**) and one mixed (**G**). The group with the mixed result was interesting because the association between LCD and SCE was significant in the direction opposite to the theory in the parametric analysis and not significant in the nonparametric one. More refined splitting of the cases into subgroups by lamina modulus and position revealed the effects of the strong interaction between the two factors. Three subgroups (**E**, **F**, and **H**) show clear, strong, and significant (in both analyses) LCD versus SCE relationships in the expected direction. However, the relationship was not significant in either analysis in the subgroup of deep and soft LCs. In addition, this figure also clearly shows some effects of the interaction between lamina modulus and position. For example, the effect of a change in lamina modulus is smaller in deep laminas (**E** versus **F**) than in shallow laminas (**H** versus **I**). Conversely, the effect of lamina depth is smaller in stiff laminas (**E** versus **H**) than that in soft laminas (**F** versus **I**). Each panel is labeled with the Pearson's product moment correlation coefficient (ρ) and Kendall's rank correlation (τ), colored *blue* if statistically significant ($P < 0.01$) or *gray* if not.

cal sensitivity in terms of LCD and SCE, it is still unknown if this translates into increased biological sensitivity and susceptibility to glaucoma.

The results and conclusions of this work are different and complementary to previous ones in the following ways: First, this study is based on eye-specific models, which incorporate charac-

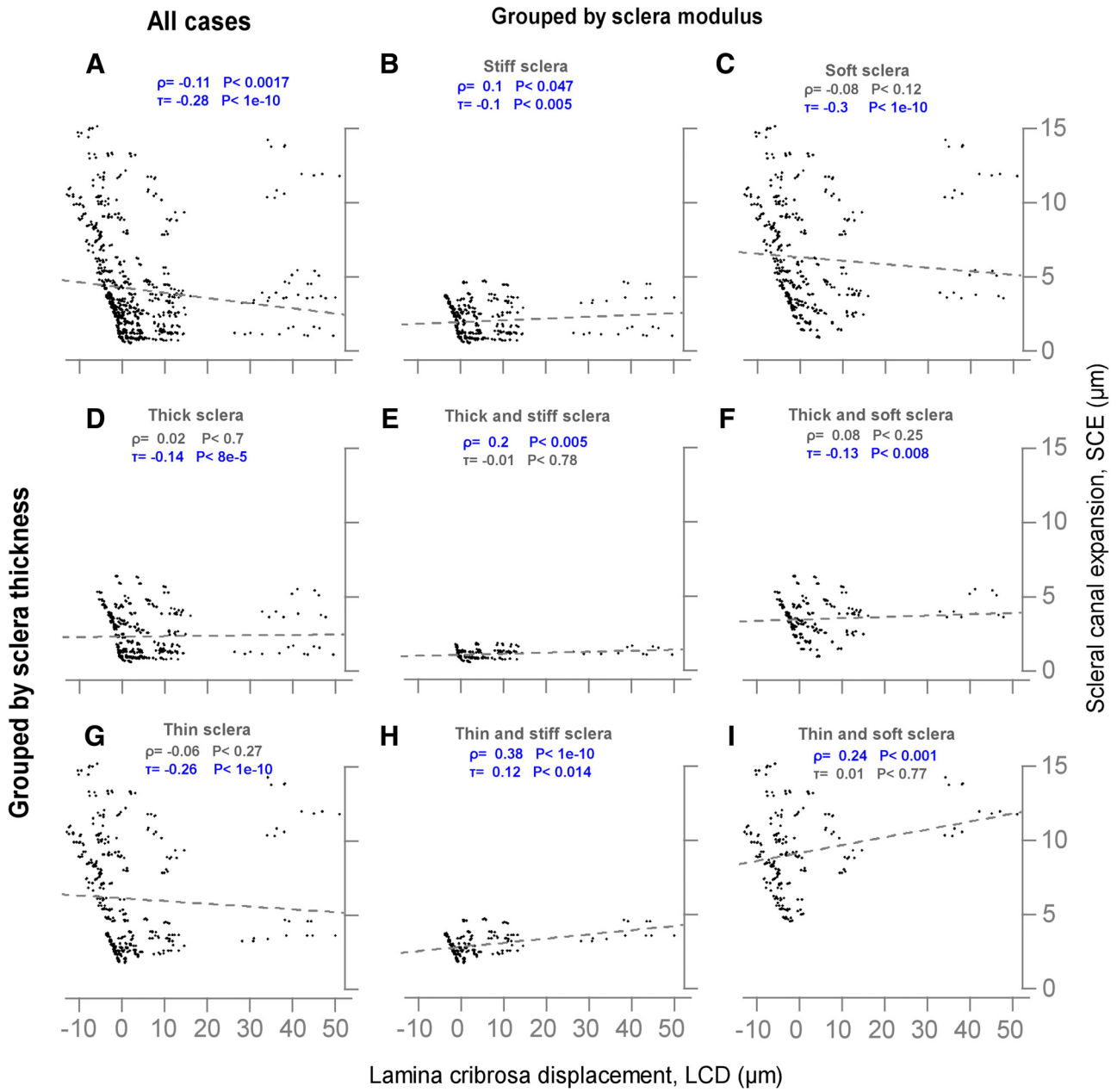

Figure 7. Scatterplot of LCD versus SCE for all cases, and for groups and subgroups split by sclera thickness and modulus. With the parametric analysis none of the subgroups shows a significant negative association between LCD and SCE, that is, consistent with the concept that "the sclera pulls the lamina taut" as IOP increases. Moreover, three of the quarter-set subgroups (**E**, **H**, and **I**) show a relationship in the direction opposite to that expected and seen on the whole (**A**). In the fourth subgroup (**F**) the relationship was not significant. This is an example of an effect called "reversal" and is an example of Simpson's paradox. The largest SCEs occurred with thin and soft sclera, whereas the smallest ones occurred with thick and stiff sclera. Interestingly, the SCEs were similar for thin and stiff sclera and thick and soft sclera, consistent with our previous application of the concept of structural stiffness.[20] Each panel is labeled with the Pearson's product moment correlation coefficient (ρ) and Kendall's rank correlation (τ), colored *blue* if statistically significant ($P < 0.01$) or *gray* if not.

teristics of the ONH that may have been missed in the generic models. Second, the parameterization techniques[23,24] (the morphing), allowed us to incorporate the effects of interactions between geometry and material properties, which have been demonstrated to be important.[12,23] Simulation studies of ONH biomechanics tend to concentrate on analyzing IOP-induced stress and strain, and often do not address LCD or SCE in as much detail. LCD and SCE are potentially clinically measurable and, therefore, a good understanding of their relationship is particularly valuable in analyzing and interpreting experiments. Another strength of this study is that we used factor ranges derived from our own measurements of the normal monkey ONH. These were compiled in a way that optimized their applicability to this study (e.g., all factors were measured in the same samples). As we have discussed elsewhere,[12,13,21,30] unnatural ranges can alter factor influences. Previous sensitivity studies used factor information from the literature, often spanning several species, treatments, and testing techniques.[12–14,30]

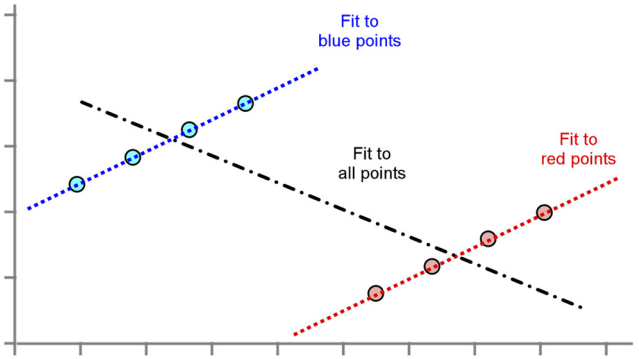

FIGURE 8. Simpson's paradox. Positive associations occur for two data groups (*blue* and *red*). When the groups are combined the association is negative. (Based on a diagram in Wikipedia: http://en.wikipedia.org/wiki/Simpson%27s_paradox; accessed on February 15, 2011).

The results in this work should be interpreted considering the assumptions, explicit or implicit, in the models and analysis. We have previously discussed issues related to the construction of the baseline models[10,11,21,23] and the choice of material properties.[10,21] Herein we present a summary of earlier discussions, with a focus on the limitations and considerations more relevant to this work. Despite being based on eye-specific geometries, the models are still simplified and do not completely reflect the complex architecture of the ONH region. We acknowledge some degree of arbitrariness in the choice of factors, particularly of the material properties. The ranges of the geometric factors are conservative since they are the ranges observed in a relatively small sample of 21 eyes. We consider our method for defining the ranges for material properties reasonable, given the information available and the assumptions on material properties (see Sigal et al.[21] for a discussion of this point). Nonetheless (see the Methods section), we evaluated the sensitivity of the results and conclusions on the assumed material ranges. Although varying the ranges slightly affected the relative influences of the factors, the main results remained consistent, showing that the results and conclusions are robust.

Also important to note is our use of a relatively small 5 mm Hg acute increase in IOP. Although this is not unprecedented,[21] it merits an explanation of our rationale: First, normal IOP is much more common than elevated IOP and, therefore, small variations in IOP are relevant to a larger group. Second, small IOP elevations may be particularly informative in understanding the pathogenesis of low-tension glaucoma. Third, as we have demonstrated here and elsewhere,[5,12,21,30,41] ONH biomechanics are complex, even with simplified geometries and material properties. Use of nonlinear or anisotropic material properties that, although approximating the true tissue behavior more closely in some cases, adds a layer of complexity that often renders the results more difficult to interpret. Simulating a relatively small IOP increase allowed us to use linear materials, whose stiffness can be specified by a single parameter for each tissue (the Young's modulus) and allowed us to refer to the tissues simply as compliant or stiff, which made the results simpler to describe. Simulating larger increases in IOP will probably necessitate the use of nonlinear material properties. Considering the tissue anisotropy, especially the circumferential fibers around the canal,[7,9,34,42–44] will make the simulations more realistic, although it is unclear how large the difference will be. Finally, we believe that providing a solid understanding of ONH biomechanics at low pressures helps build to an understanding of larger pressure increases. The models represent an acute deformation of the tissues due to increases in IOP and do not account for viscoelastic effects or tissue remodeling. The consequences of introducing these complexities are difficult to predict because their effects are nonlinear and depend on interacting factors. We are working on models with more realistic material properties (inhomogeneous, nonlinear and anisotropic sclera,[7,9,34,45–48] and lamina cribrosa[9–11,17,32,42,43,46,49]) and techniques to simulate connective tissue remodeling.[35,49–51] The models presented here did not consider the loadings due to cerebrospinal fluid pressure, which may also affect laminar biomechanics.[52,53]

We evaluated the relationship between LCD and SCE with both parametric (Pearson's product moment correlation) and nonparametric (Kendall's rank correlation) methods. We decided to include the results of the parametric analyses because the conclusions derived using the parametric analyses were essentially the same as those obtained using nonparametric methods, and because the linear regression associated with the linear analysis is simple to visualize.

In summary, we have used numerical techniques to study the association between the anterior–posterior LCD and the SCE associated with acute changes in IOP. We found that the association between these two aspects of the ONH response to increases in IOP varied. For some conditions, such as deep and stiff lamina, it was strong and negative (lamina displacing anteriorly under increased IOP). For other conditions, such as shallow and compliant lamina, the association was not there. Furthermore, for thin and stiff sclera it was weak and positive (lamina displacing posteriorly under increased IOP). In this work we have laid the foundation for understanding the relationship between elements of the response of the ONH to increases in IOP, and how this depends on the properties of the rest of the globe. Our intention was to provide the ophthalmology community with a foundation for a solid understanding of the complex interactions underlying the effects of acute IOP variations.

APPENDIX

Summary of Factor and Interaction Influences Identified in Sigal et al.[21] (Fig. A1)

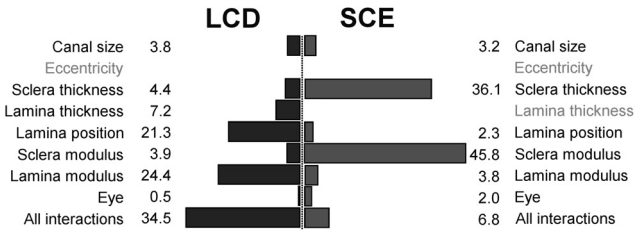

FIGURE A1. Relative influences of all factors and interactions. Percentage contributions of the factors and interactions to the sum of squares corrected by the mean, as a measure of relative influence. The bar lengths are proportional to the numbers and are intended to simplify seeing the influences at a glance. Factors with a statistically significant effect ($P < 0.01$) are shown in *black*, the rest in *gray*. The influential factors were different for each response: LCD was most influenced by lamina position and modulus, whereas SCE was most influenced by scleral thickness and modulus. Both LCD and SCE were influenced by interactions, LCD more strongly than SCE. Recall that interactions may be interpreted as curvature in response space. Thus, even relatively small contributions to the sum of squares may represent a large effect on the actual response. Simplified from Sigal et al.[21]

Acknowledgments

The authors thank Juan Reynaud for his contributions in preprocessing the source data.

References

1. Quigley HA. Number of people with glaucoma worldwide. *Br J Ophthalmol.* 1996;80:389–393.
2. Minckler DS, Bunt AH, Johanson GW. Orthograde and retrograde axoplasmic transport during acute ocular hypertension in the monkey. *Invest Ophthalmol Vis Sci.* 1977;16:426–441.
3. Quigley HA. Glaucoma: macrocosm to microcosm (The Friedenwald Lecture). *Invest Ophthalmol Vis Sci.* 2005;46:2662–2670.
4. Burgoyne CF, Downs JC, Bellezza AJ, Suh JK, Hart RT. The optic nerve head as a biomechanical structure: a new paradigm for understanding the role of IOP-related stress and strain in the pathophysiology of glaucomatous optic nerve head damage. *Prog Retin Eye Res.* 2005;24:39–73.
5. Sigal IA, Ethier CR. Biomechanics of the optic nerve head. *Exp Eye Res.* 2009;88:799–807.
6. Azuara-Blanco A, Costa VP, Wilson RP. *Handbook of Glaucoma.* Singapore: Taylor & Francis; 2001:280.
7. Girard MJA, Suh J-KF, Bottlang M, Burgoyne CF, Downs JC. Scleral biomechanics in the aging monkey eye. *Invest Ophthalmol Vis Sci.* 2009;50:5226–5237.
8. Girard MJA, Suh J-KF, Bottlang M, Burgoyne CF, Downs JC. Biomechanical changes in the sclera of monkey eyes exposed to chronic IOP elevations. *Invest Ophthalmol Vis Sci.* 2011 ;52 :5656–5669.
9. Grytz R, Meschke G, Jonas JB. The collagen fibril architecture in the lamina cribrosa and peripapillary sclera predicted by a computational remodeling approach. *Biomech Model Mechanobiol.* 2011;10:371–382.
10. Roberts MD, Liang Y, Sigal IA, et al. Correlation between local stress and strain and lamina cribrosa connective tissue volume fraction in normal monkey eyes. *Invest Ophthalmol Vis Sci.* 2010; 51:295–307.
11. Roberts MD, Sigal IA, Liang Y, Burgoyne CF, Downs JC. Changes in the biomechanical response of the optic nerve head in early experimental glaucoma. *Invest Ophthalmol Vis Sci.* 2010;51: 5675–5684.
12. Sigal IA. Interactions between geometry and mechanical properties on the optic nerve head. *Invest Ophthalmol Vis Sci.* 2009;50: 2785–2795.
13. Sigal IA, Flanagan JG, Ethier CR. Factors influencing optic nerve head biomechanics. *Invest Ophthalmol Vis Sci.* 2005;46:4189–4199.
14. Sigal IA, Flanagan JG, Tertinegg I, Ethier CR. Finite element modeling of optic nerve head biomechanics. *Invest Ophthalmol Vis Sci.* 2004;45:4378–4387.
15. Agoumi Y, Sharpe GP, Hutchison DM, Nicolela MT, Artes PH, Chauhan BC. Laminar and prelaminar tissue displacement during intraocular pressure elevation in glaucoma patients and healthy controls. *Ophthalmology.* 2011;118:52–59.
16. Yan DB, Coloma FM, Metheetrairut A, Trope GE, Heathcote JG, Ethier CR. Deformation of the lamina cribrosa by elevated intraocular pressure. *Br J Ophthalmol.* 1994;78:643–648.
17. Yang H, Downs JC, Sigal IA, Roberts MD, Thompson H, Burgoyne CF. Deformation of the normal monkey optic nerve head connective tissue after acute IOP elevation within 3-D histomorphometric reconstructions. *Invest Ophthalmol Vis Sci.* 2009;50:5785–5799.
18. Bellezza AJ, Rintalan CJ, Thompson HW, Downs JC, Hart RT, Burgoyne CF. Anterior scleral canal geometry in pressurised (IOP 10) and non-pressurised (IOP 0) normal monkey eyes. *Br J Ophthalmol* 2003;87:1284–1290.
19. Levy NS, Crapps EE, Bonney RC. Displacement of the optic nerve head. Response to acute intraocular pressure elevation in primate eyes. *Arch Ophthalmol.* 1981;99:2166–2174.
20. Strouthidis NG, Fortune B, Yang H, Sigal IA, Burgoyne CF. The effect of acute intraocular pressure elevation on the monkey optic nerve head as detected by spectral domain optical coherence tomography. *Invest Ophthalmol Vis Sci.* In press.
21. Sigal IA, Yang H, Roberts MD, Burgoyne CF, Downs JC. IOP-induced lamina cribrosa displacement and scleral canal expansion: an analysis of factor interactions using parameterized eye-specific models. *Invest Ophthalmol Vis Sci.* 2011;52:1896–1907.
22. Sigal IA, Flanagan JG, Tertinegg I, Ethier CR. Modeling individual-specific human optic nerve head biomechanics. Part I: IOP-induced deformations and influence of geometry. *Biomech Model Mechanobiol.* 2009;8:85–98.
23. Sigal IA, Yang H, Roberts MD, Downs JC. Morphing methods to parameterize specimen-specific finite element model geometries. *J Biomech.* 2010;43:254–262.
24. Sigal IA, Hardisty MR, Whyne CM. Mesh-morphing algorithms for specimen-specific finite element modeling. *J Biomech.* 2008;41: 1381–1389.
25. Anderson MJ, Whitcomb PJ. *DOE Simplified: Practical Tools for Effective Experimentation*. New York: Productivity Press; 2000: 256.
26. Montgomery DC. *Design and Analysis of Experiments.* Hoboken, NJ: Wiley; 2004:660.
27. Yang H, Downs JC, Bellezza A, Thompson H, Burgoyne CF. 3-D histomorphometry of the normal and early glaucomatous monkey optic nerve head: prelaminar neural tissues and cupping. *Invest Ophthalmol Vis Sci.* 2007;48:5068–5084.
28. Yang H, Downs JC, Burgoyne CF. Physiologic intereye differences in monkey optic nerve head architecture and their relation to changes in early experimental glaucoma. *Invest Ophthalmol Vis Sci.* 2009;50:224–234.
29. Yang H, Downs JC, Girkin C, et al. 3-D histomorphometry of the normal and early glaucomatous monkey optic nerve head: lamina cribrosa and peripapillary scleral position and thickness. *Invest Ophthalmol Vis Sci.* 2007;48:4597–4607.
30. Sigal IA, Flanagan JG, Tertinegg I, Ethier CR. Modeling individual-specific human optic nerve head biomechanics. Part II. Influence of material properties. *Biomech Model Mechanobiol.* 2009;8:99–109.
31. Sander EA, Downs JC, Hart RT, Burgoyne CF, Nauman EA. A cellular solid model of the lamina cribrosa: mechanical dependence on morphology. *J Biomech Eng.* 2006;128:879–889.
32. Roberts MD, Grau V, Grimm J, et al. Remodeling of the connective tissue microarchitecture of the lamina cribrosa in early experimental glaucoma. *Invest Ophthalmol Vis Sci.* 2009;50:681–690.
33. Downs JC, Suh JK, Thomas KA, Bellezza AJ, Hart RT, Burgoyne CF. Viscoelastic material properties of the peripapillary sclera in normal and early-glaucoma monkey eyes. *Invest Ophthalmol Vis Sci.* 2005;46:540–546.
34. Girard MJ, Downs JC, Bottlang M, Burgoyne CF, Suh JK. Peripapillary and posterior scleral mechanics—Part II: experimental and inverse finite element characterization. *J Biomech Eng.* 2009;131: 051012.
35. Sigal IA, Flanagan JG, Tertinegg I, Ethier CR. 3D morphometry of the human optic nerve head. *Exp Eye Res.* 2010;90:70–80.
36. Morgan WH, Chauhan BC, Yu DY, Cringle SJ, Alder VA, House PH. Optic disc movement with variations in intraocular and cerebrospinal fluid pressure. *Invest Ophthalmol Vis Sci.* 2002;43:3236–3242.
37. Sigal IA, Flanagan JG, Tertinegg I, Ethier CR. Predicted extension, compression and shearing of optic nerve head tissues. *Exp Eye Res.* 2007;85:312–322.
38. Baker SG, Kramer BS. Good for women, good for men, bad for people: Simpson's paradox and the importance of sex-specific analysis in observational studies. *J Womens Health Gend Based Med.* 2001;10:867–872.
39. Hernán MA, Clayton D, Keiding N. The Simpson's paradox unraveled. *Int J Epidemiol.* 2011;40:780–785.
40. Wagner CH. Simpson's paradox in real life. *Am Statistician.* 1982; 36:46–48.
41. Roberts MD, Hart RT, Liang Y, Bellezza A, Burgoyne CF, Downs J. Continuum-level finite element modeling of the optic nerve head using a fabric tensor based description of the lamina cribrosa. *ASME Summer Bioengineering Conference*. Keystone, CO: American Society of Mechanical Engineers; 2007.

42. Morishige N, Wahlert AJ, Kenney MC, et al. Second-harmonic imaging microscopy of normal human and keratoconus cornea. *Invest Ophthalmol Vis Sci*. 2007;48:1087–1094.
43. Winkler M, Jester B, Nien-Shy C, et al. High resolution three-dimensional reconstruction of the collagenous matrix of the human optic nerve head. *Brain Res Bull*. 2010;81:339–348.
44. Quigley HA, Dorman-Pease ME, Brown AE. Quantitative study of collagen and elastin of the optic nerve head and sclera in human and experimental monkey glaucoma. *Curr Eye Res.* 1991;10:877–888.
45. Yan D, McPheeters S, Johnson G, Utzinger U, Vande Geest JP. Microstructural differences in the human posterior sclera as a function of age and race. *Invest Ophthalmol Vis Sci.* 2011;52:821–829.
46. Grytz R, Meschke G. A computational remodeling approach to predict the physiological architecture of the collagen fibril network in corneo-scleral shells. *Biomech Model Mechanobiol.* 2010; 9:225–235.
47. Woo SL, Kobayashi AS, Schlegel WA, Lawrence C. Nonlinear material properties of intact cornea and sclera. *Exp Eye Res.* 1972; 14:29–39.
48. Myers KM, Cone FE, Quigley HA, Gelman S, Pease ME, Nguyen TD. The in vitro inflation response of mouse sclera. *Exp Eye Res*. 2010;91:866–875.
49. Grytz R, Sigal IA, Ruberti JW, Meschke G, Downs JC. Lamina cribrosa thickening in early glaucoma predicted by a microstructure motivated growth and remodeling approach. *Mech Mater*. In press.
50. Sigal IA, Yang H, Roberts MD, Burgoyne CF, Downs JC. Biomechanics of the posterior pole during remodeling progression from normal to early experimental glaucoma. *ASME 2009 Summer Bioengineering Conference*. Lake Tahoe, CA: American Society of Mechanical Engineers; 2009.
51. Yang H, Williams G, Downs JC, et al. Posterior (outward) migration of the lamina cribrosa and early cupping in monkey experimental glaucoma. *Invest Ophthalmol Vis Sci*. 2011;52:7109–7121.
52. Berdahl JP, Allingham RR, Johnson DH. Cerebrospinal fluid pressure is decreased in primary open-angle glaucoma. *Ophthalmology.* 2008;115:763–768.
53. Ren R, Jonas JB, Tian G, et al. Cerebrospinal fluid pressure in glaucoma: a prospective study. *Ophthalmology.* 2010;117:259–266.